



# Membrane electrode assembly with enhanced platinum utilization for high temperature proton exchange membrane fuel cell prepared by catalyst coating membrane method



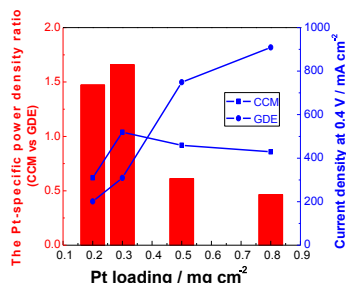
Huagen Liang, Huaneng Su\*, Bruno G. Pollet, Vladimir Linkov, Sivakumar Pasupathi

HySA Systems Competence Centre, South African Institute for Advanced Materials Chemistry, University of the Western Cape, Private Bag X17, Bellville 7535, South Africa

## HIGHLIGHTS

- Low Pt loading MEAs for HT-PEMFC were prepared by CCM method.
- The CCM-based MEAs showed enhanced Pt utilization compared to GDEs at low Pt loading.
- Cell resistances can be decreased by CCM method at low Pt loading.
- Enhanced electrochemical surface area was obtained with CCM at low Pt loading.

## GRAPHICAL ABSTRACT



## ARTICLE INFO

### Article history:

Received 29 January 2014

Received in revised form

9 April 2014

Accepted 4 May 2014

Available online 14 May 2014

### Keywords:

High temperature proton exchange membrane fuel cell  
Membrane electrode assembly  
Catalyst coating membrane  
Pt utilization

## ABSTRACT

In this work, membrane electrode assemblies (MEAs) prepared by catalyst coating membrane (CCM) method are investigated for reduced platinum (Pt) loading and improved Pt utilization of high temperature proton exchange membrane fuel cell (PEMFC) based on phosphoric acid (PA)-doped poly(2,5-benzimidazole) (AB-PBI) membrane. The results show that CCM method exhibits significantly higher cell performance and Pt-specific power density than that of MEAs prepared with conventional gas diffusion electrode (GDE) under a low Pt loading level. In-suit cyclic voltammetry (CV) and electrochemical impedance spectroscopy (EIS) show that the MEAs prepared by the CCM method have a higher electrochemical surface area (ECSA), low cell ohmic resistance and low charge transfer resistance as compared to those prepared with GDEs at the same Pt loading.

© 2014 Elsevier B.V. All rights reserved.

## 1. Introduction

Compared to the low temperature fuel cells, the phosphoric acid (PA) doped polybenzimidazole (PBI) membrane based high-temperature proton exchange membrane fuel cells (HT-PEMFC) exhibit several unique advantages: excellent CO tolerance, enhance electrode reactions with especial relevance in the case of

oxygen reduction reaction, no-dependency on intricate water management, higher utilization of residual heat and simple system without humidification system [1–3]. Hence, they are considered to be the promising energy conversion device and have attracted enormous attention in the last decades [1–6]. Membrane electrode assembly (MEA) is the most critical component of PEMFCs, which is comprised of anode and cathode catalyst layers (CL), gas diffusion layers (GDL) and proton exchange membrane (for PBI-based HT-PEMFC, proton conduction is rely on the PA doping level). The cell performance directly depends on the properties of the MEA [7–9].

\* Corresponding author. Tel./fax: +27 21 9599310.  
E-mail address: [suhuaneng@gmail.com](mailto:suhuaneng@gmail.com) (H. Su).

So far, MEAs for the PA doped PBI membrane based HT-PEMFCs were prepared by spraying catalyst inks on the surface of GDL with microporous layer (MPL) followed by hot-pressing, which is known as gas diffusion electrode (GDE) method [4–6,10–15]. This method is appropriate to fabricate the large-scale MEA and for mass production [9]. However, there may be a lot of Pt/C nanoparticles immersed into the gap of GDL, resulting in the waste of catalyst [16]. In addition, the contact between the CL and the membrane was weak due to the CL was combined with the GDL. Therefore, the interfacial resistances between the membrane and CLs could be high.

In the research of Nafion® based low temperature PEM fuel cell, MEAs were commonly fabricated by catalyst coated membrane (CCM) method, in which the CLs were directly coated on the surface of the membrane, the results indicated that CCM method can enhance the catalyst utilization efficiency and decrease the interface resistance between the CLs and the membrane compared to GDE method [17–20]. However, this method was seldom used to prepare MEAs for HT-PEMFCs due to the problems caused by introducing PA into the PBI membranes of the CCMs. When a pre-doped membrane is used for CCM, the surface of the membrane tends to keep wet even at high temperature because of the exudation and the strong moisture absorption of PA, which results the catalyst powder cannot effectively attach with the membrane. Possibly for this reason, Cho et al. [21] prepared a CCM with dry PBI membrane and then soaked it in 85% PA solution to doping enough PA in the membrane. Although a higher performance was observed in their work with this PA-doped CCM, it is very risky because the intense swelling of the PBI membrane due to the high acid uptake could cause serious dimensional change of the coated CL. Moreover, the CCM could serious distort due to the different PA absorption rates between the CL covered membrane and the bare membrane around, resulting in detachment of the CL and difficulties in MEA.

Recently, Wannek et al. [22] reported a novel strategy for introducing PA into HT-PEMFCs by using acid impregnated CLs instead of pre-doped membranes. They proved that the redistribution of PA in MEAs is a rather quick process whether PA is doped in the GDEs or pre-doped inside the membrane, which makes the use of un-doped PBI membranes for HT-PEMFCs possible. Inspired by their findings, we developed a novel method to prepare CCM-based MEAs for HT-PEMFCs by acid impregnated GDLs instead of pre-doped CCMs, through this way the deformation of the CCM can be suppressed and the integration of the CLs can be maintained. The performance and electrochemical properties of this MEA were characterized under normal operating conditions with different Pt loadings, and the availability of this CCM method was discussed.

## 2. Experimental

The membranes used in this study are AB-PBI (=poly(2,5-benzimidazole)), which were supplied by FuMA-Tech (fuma-pem®AM, ~50 µm). Commercial Hispec4000 Pt/C (40 wt.% Pt, Johnson Matthey) was used for the CCM preparation, and the catalyst inks were mixed by adding catalyst and 5 wt.% PVDF/DMAc solution into the extra DMAc solvent. Before preparing the CLs, a homogeneous suspension of the catalyst inks was ultrasonicated for 50 min at room temperature. The dry PVDF content in the CL was adjusted to be 15 wt.%. In this work, we prepared and investigated a series of CCMs with different cathode Pt loadings of 0.2, 0.3, 0.5, 0.8 mg cm<sup>-2</sup>, respectively. The Pt loadings of anodes were fixed at 0.5 mg cm<sup>-2</sup>. The actual electrode area of the MEAs in this study was 2.3 × 2.3 cm<sup>2</sup>.

### 2.1. Preparation of membrane electrode assemblies

All the MEAs were established by using an automated ultrasonic spraying machine (Ultrasonic Spray Coating System, SonoTEK Corporation, USA). For the fabrication of CCM and GDE, the catalyst inks were uniformly sprayed onto the dry AB-PBI membranes (for CCMs) or on the MPL (for GDEs) of a commercially available GDL (H2315-CX196, Freudenberg, Germany). In order to make the solvent evaporated quickly during the spraying process, the membranes or GDLs were fixed on a 100 °C plate. The resulting CCMs or GDEs were dried at 140 °C under vacuum overnight to remove residual DMAc solvents.

For the GDE-type MEA, the PA-doping process was performed by immersing the membranes in 85% PA solution at 100 °C for 24 h, which gave the membrane an acid doping level of about 3.8 molecules of H<sub>3</sub>PO<sub>4</sub> per polymer repeating unit [4–6]. For the CCM-type MEAs, the introduction of PA was conducted by impregnating the GDLs with predefined amounts of PA. A H<sub>3</sub>PO<sub>4</sub>/ethanol solution (0.2 mg µl<sup>-1</sup>) was evenly dropped onto the top of commercial GDLs by several times. Afterwards the ethanol was allowed to evaporate overnight in an oven at 80 °C. The amount of PA pre-impregnated in the GDLs was calculated by the weight of the dry membrane (before CL coating) with the actual electrode area. Similarly, the PA doping level is also about 3.8 molecules of H<sub>3</sub>PO<sub>4</sub> per polymer repeating unit with the actual electrode area.

### 2.2. Single-cell tests

The CCM- or GDE-based MEAs were assembled in a single cell fixture (BalticFuelCellsGmbH, Germany) together with fluorinated polymer gaskets without hot-press. This test cell consists of graphite plates with single serpentine gas channels and solid metallic endplates equipped with heating cartridges and then connected to a Cell Compression Unit (Pragma Industries, France). The cell performances were evaluated at 160 °C and under ambient pressure using an in-house HT-PEMFC setup, which consisted of a PC loaded with Labview software to control the electronic load (Höcherl&Hackl GmbH, Germany) and mass flow controllers (Bronkhorst, Netherlands). Pure hydrogen and compressed air were fed to the anode and cathode, respectively, at flow rates of 200 and 1000 mL min<sup>-1</sup>. Before the polarization curve test, the cells were activated at 0.5 V and 160 °C until stable performance was obtained. The current–voltage polarization curves were obtained by measuring the voltage with stepwise increment of current density from 0 to 2000 mA cm<sup>-2</sup> with intervals of 20 mA cm<sup>-2</sup>, until the cell voltage approaches 0.2 V. At each current, the cell voltage was measured after a hold time of 2 min to allow the cell approaching steady state. For accuracy, single cell tests on each MEA prepared by CCM method or GDE with different Pt loading were performed at least three times, and then the average values (voltage) were determined. Normally, the relative standard deviations of these values were less than 4%.

### 2.3. Electrochemical measurements

Electrochemical impedance spectroscopy (EIS) and cyclic voltammetry (CV) were performed using an Autolab PGSTAT 30Potentiostat/Galvanostat (Metrohm) equipped with a 20 A booster and a frequency response analysis (FRA) module. To determine the resistance of the MEAs, the *in-suit* EIS were conducted at 0.6 V in potentiostatic mode. A signal amplitude of 5 mV in the frequency range of 100 mHz–20000 Hz was applied. Because of the much faster reaction kinetics of the H<sub>2</sub> oxidation reaction on the Pt electrocatalysts as compared to that of the O<sub>2</sub> reduction reaction, the cell impedance would be mainly dominated by the

cathodic impedance for the  $O_2$  reduction reaction. The anode at which hydrogen oxidation takes place was used as the reference and also as the counter electrode, while the cathode was used as the working electrode [7].

Cyclic voltammetry (CV) measurements were conducted at  $160^\circ C$  to study the electrochemically active surface area (ECSA) using dry  $N_2$  at the cathode (working electrode) and dry  $H_2$  at the anode (counter electrode and reference electrode). The potential was scanned from 0 V to 1.2 V at a sweep rate of  $0.05 V s^{-1}$ . For better accuracy, CV measurements of each MEA were performed at least three times during the polarization curves testing. Normally, the relative standard deviations of these ECSAs were less than 5%.

### 3. Results and discussion

In the PBI-based high temperature PEMFC, PA is usually used as the proton conductor within the membrane and the CLs [23]. With the reaction occurring in the CLs, there exists a dynamic exchange of PA between the membrane and the CLs. In addition, AB-PBI membrane can easily absorb large amounts of water and especially PA like other polybenzimidazoles [22]. For preparation of MEA by CCM method, the PA is impregnated in the GDLs. It means that PA transfers from the GDLs to the CCM during the cell operation. Fig. 1 shows the photographs of a fresh CCM (Fig. 1(a)) and the CCM after testing (Fig. 1(b)), the GDLs were peeled off. It is clear that PA redistribution mainly happened around the actual electrode area, and no serious swelling or distortion occurred after test as the dimension of the tested CCM almost kept same with the original (Fig. 1(a)). According to Wennek et al. [22], a part of these PA will be transferred to the membrane, combining with AB-PBI units. Others will serve as “free PA” to reach a dynamic equilibrium in the membrane and the CLs for proton conduction. It is believed that a majority of PA will be concentrated in the membrane and the adjacent CLs, due to the good affinity of the AB-PBI membrane and the transportation of the protons. It was found that the redistribution of PA in HT-PEFC MEAs prepared by PA doped GDEs and a dry AB-PBI membrane is a rather quick process and moderate current densities can be achieved in only about 10 min after cell start-up [22]. Although it takes several hours until a dynamic equilibrium of the acid distribution is reached, the amount of PA transferred to the membrane within the very first minutes of cell operation is high enough to result in a substantial proton conductivity [22].

The polarization curves and Pt-specific power density of MEAs prepared by CCMs and GDEs with different Pt loadings are presented in Fig. 2, respectively. From Fig. 2(a), it can be observed that the performance of MEA with  $0.2 mg cm^{-2}$  Pt is slightly better than that of other MEAs in the low current density region

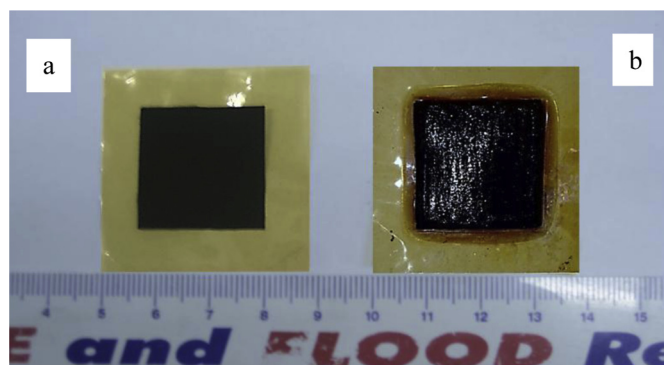


Fig. 1. Digital photos of CCM-based MEA before (a) and after (b) testing.

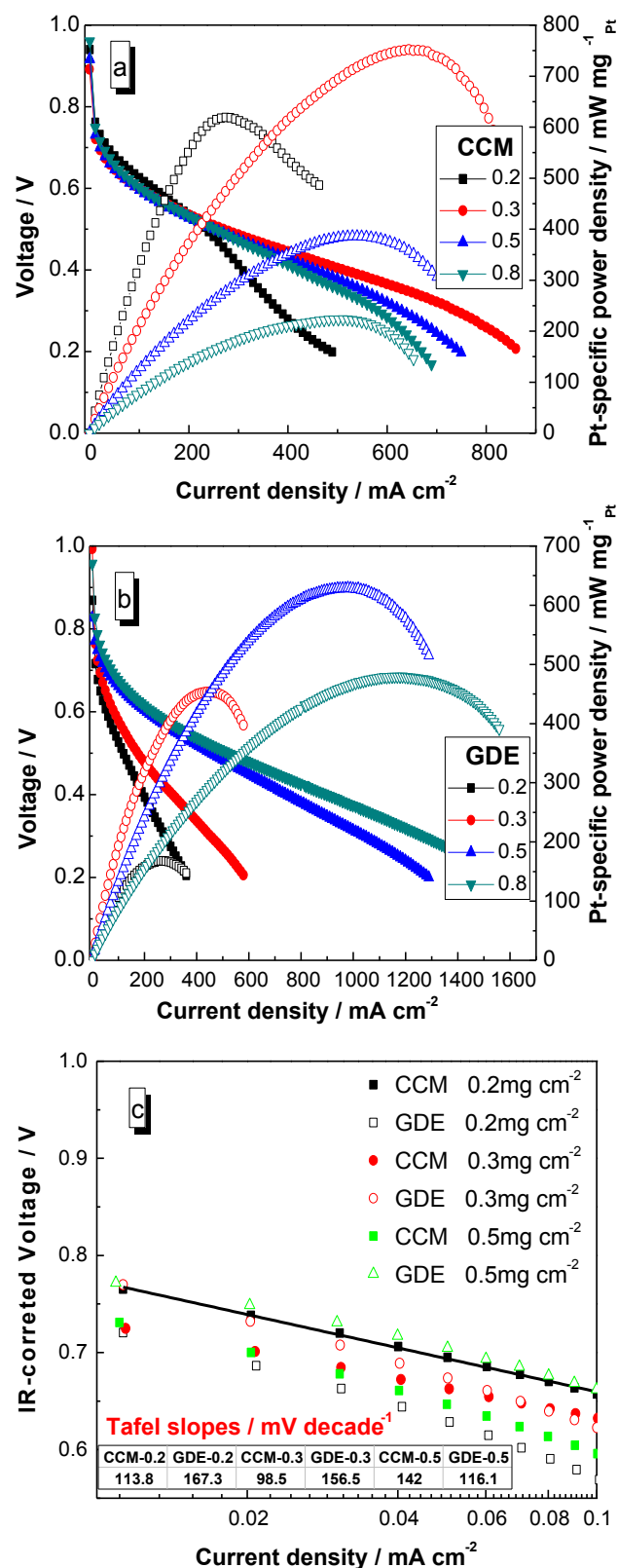


Fig. 2. Cell performances of MEAs fabricated by CCM (a) and GDE (b) method with different Pt loading for anode and cathode and the Tafel slope (c) fitted from the IR-free polarization curves.

(<200 mA cm<sup>-2</sup>). The ohmic resistance of MEA was influenced seriously by the amount of PA in the AB-PBI membrane. Since the PA doping level is same in each MEA, the amount of PA absorbed in the membrane may be more for MEA with only 0.2 mg cm<sup>-2</sup> Pt loading than the other MEAs. Furthermore, a thinner CL means less electronic resistance. Hence, a lower ohmic resistance of the single cell and a better performance can be achieved in this region. Nevertheless, the entirely cell performance decreases with the Pt loading further increased from 0.3 to 0.8 mg cm<sup>-2</sup>. In GDE-based MEAs, the AB-PBI membranes were pre-doped with PA, a small amount of PA can diffuse into the CLs as required electrolyte for proton transfer, which has no serious effect on O<sub>2</sub> transport, because the GDLs and the outer CL would not be blocked by the small amount of PA. So better MEA performance can be obtained with higher Pt loading. However, for CCM-based MEAs, the great amount of PA were pre-impregnated in the GDLs. If the CLs are thick, the PA diffusion from GDL to ABPBI membrane may difficult even the membrane has strong affinity with PA. The residual PA in the GDLs and the CLs may great higher than that for GDE-based MEAs, resulting in difficulties in O<sub>2</sub> diffusion, resulting in performance deterioration in the high current density region.

For the CCM with the cathode Pt loading of 0.3 mg cm<sup>-2</sup>, the limiting current density can reach 850 mA cm<sup>-2</sup> and the maximum Pt-specific power density is ~760 mW mg<sup>-1</sup> Pt. From Fig. 3, it can be seen that the difference of current density at 0.4 V is tiny when the Pt loading increased from 0.5 mg cm<sup>-2</sup> to 0.8 mg cm<sup>-2</sup>, which implies further increasing Pt loading is not helpful to improve the cell performance.

As shown in Fig. 2(b), it can be seen that the performances of GDEs are worse than that of CCM-based MEAs while the Pt loading is only 0.2 and 0.3 mg cm<sup>-2</sup>. At 0.6 V, the current density of the CCM-based MEA with 0.2 mg cm<sup>-2</sup> and 0.3 mg cm<sup>-2</sup> Pt loading is 120 mA cm<sup>-2</sup> and 100 mA cm<sup>-2</sup>, respectively, while the values for the GDE-based MEA are only 50 mA cm<sup>-2</sup> and 80 mA cm<sup>-2</sup>. From Fig. 2(c), the Tafel slope can be fitted from the IR-free polarization curves. For the MEAs prepared by GDEs, the Tafel slope is 167.3, 156.5 and 116.1 mV decade<sup>-1</sup>, respectively. However, a significant reduce can be observed for using CCM method at lower Pt loading (like 0.2, 0.3 mg cm<sup>-2</sup>), which is attribute to higher kinetics of oxygen reduction reaction at the cathode for CCM-based MEAs [7]. Surprisingly, the CCM-based MEA shows higher Tafel slope than GDE-based MEA at 0.5 mg cm<sup>-2</sup> Pt loading. According to Perry et al. [24], if the change of CL structure leads to different reaction paths or

limiting cases, the Tafel slope could change even the CL materials and the temperature of the reaction sites are same. In our case, the PA diffusion and CL/membrane interface contact are different because the different CL depositing mode, then the surroundings of the reaction sites may be changed due to the change of PA distribution and Pt/AB-PBI membrane interaction, which may lead to a change in the ORR path or limiting case, then causing the change of Tafel slope. When the CL is thin (low Pt loading, like 0.2 and 0.3 mg cm<sup>-2</sup>), the PA distribution in the CL of CCM should be similar with that of GDE, then the kinetics of the CL is mainly dominated by CL/membrane interface conditions. It is generally considered that CCM has superior CL/membrane interface, which may be the reason why CCM shows better ORR kinetics than GDE at low Pt loadings. In contrast, when the CL is thick (higher Pt loading, like 0.5 and 0.8 mg cm<sup>-2</sup>), the PA distribution in the CL of CCM could be very different with that of GDE due to the different PA doping method. The PA pre-impregnated in the GDL must go through the whole CL before being absorbed by the membrane, which may cause higher anions adsorption on Pt surface than that for GDE, in which only small amount of PA can diffuse into the CL as required electrolyte. That's may be the reason CCM shows inferior ORR kinetics at higher Pt loading of 0.5 mg cm<sup>-2</sup>.

Compared the Pt-specific power density (measured in cathode Pt-specific power density) at low Pt loading, it is clear that the CCM-based MEA shows higher Pt-specific power density than that of the GDE-based MEA probably due to the reduced catalyst loss into the gap on the surface of GDL and improved CL/membrane interfacial contact. The Pt-specific power density ratio of CCM to GDE can reach up to 1.7 times at 0.3 mg cm<sup>-2</sup> Pt (Fig. 3). We suggest that the highest Pt-specific power density received at 0.3 mg cm<sup>-2</sup> can be ascribed to the combination of better kinetics of the ORR and good mass transfer ability. And it can be seen that the highest Pt-specific power density of each MEA is received at the high current density region. It should be noted that the way of introducing PA for CCM-based MEAs is different with that for GDE-based MEAs. In GDE-based MEAs, the required PA for proton transfer relies on the PA diffusion from pre-doped PBI membrane while the PA in the CCM-based MEAs comes from their PA impregnated GDLs. The PA must go through the whole CL before being absorbed by the membrane. The residual PA in the GDLs and the CLs may great higher than that for GDE-based MEAs, which could also cause difficulties in O<sub>2</sub> diffusion, resulting in performance deterioration, especially when the CL is thick. Therefore, we suggest that the diffusion of oxygen for the GDE-based MEA is preferable to that in the CCM-based MEA as the risk of PA flood in the CLs should much lower for the former. Hence, from Fig. 2(b), it can be seen that the performance of GDE-based MEAs are much better than that of CCM-based MEAs at higher Pt loadings. The limiting current density of the GDE-based MEA with 0.8 mg cm<sup>-2</sup> Pt loading can reach up to 1600 mA cm<sup>-2</sup>, which is almost twice than that of the CCM-based MEA with the same Pt loading.

In order to further understand the effect of the MEA type on the cell performance, the EIS measurements were conducted at cell potential of 0.6 V and at 160 °C. Fig. 4 shows the *in-situ* impedance curves and Fig. 5 is the equivalent circuit used for fitting. It is clear that a satisfactory agreement between the marked points measured from the experiment and the solid lines fitted based on the equivalent circuit, indicating the validity of the equivalent circuit model.

In the equivalent circuit model,  $R_0$  represents the total ohmic resistance of the cell which includes the ohmic resistances of the membrane and the electrodes, the contact resistances between various cell components, was measured from the intercept at the real axis of the high frequency (as shown in Fig. 4). Generally, two semicircle scan be seen on the spectrum for the high temperature

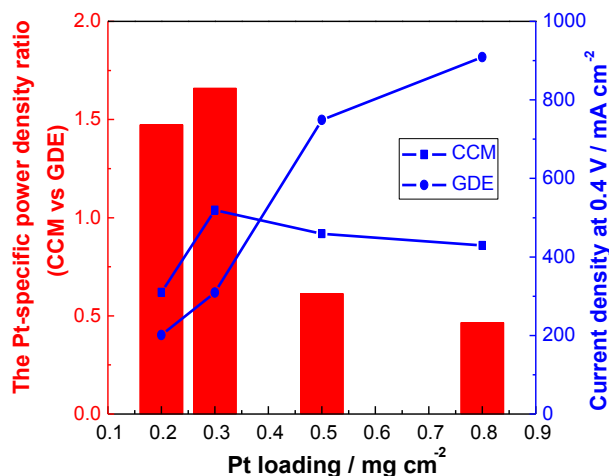


Fig. 3. The Pt utilization ratio and the current density at 0.4 V comparison of MEAs prepared by CCM and GDE.

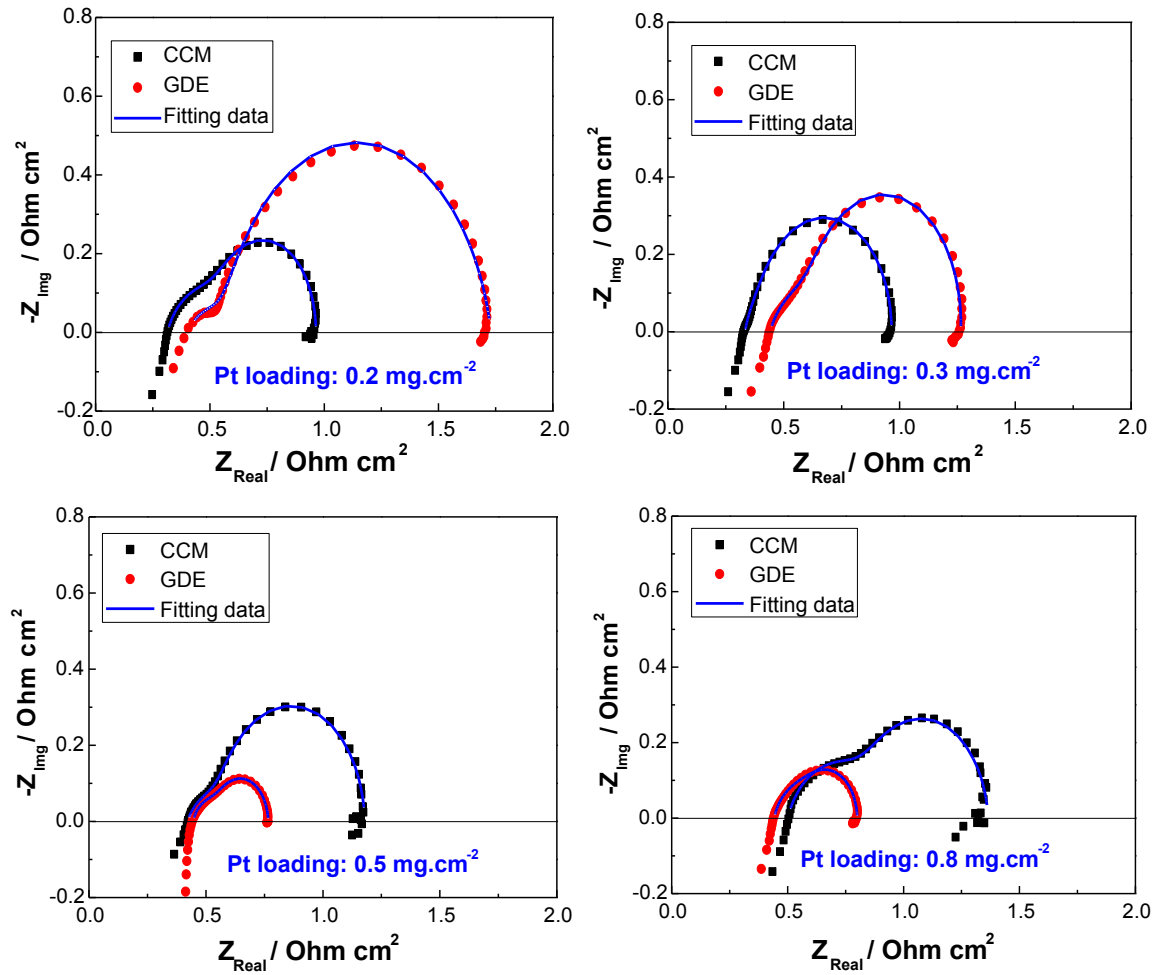


Fig. 4. Impedance curves of single cells using MEAs prepared by different method, measured at 0.6 V and 160 °C.

PEMFC [25–27]. The tiny semicircle at the high frequency section related to  $R_a$  represents the coupling of the distributed ionic resistance and capacitance in the CL [26], which is influenced by the MEA structure, high-frequency relaxation to the distributed resistance effects in the CL, or the contact capacitance in the electrode structure [25]. The larger semicircle at low frequency section related to  $R_c$  represents the charge transfer resistance across the catalyst/electrolyte interface in the CL (linked to the kinetic of the electrochemical reaction) [26,28]. Because the reaction kinetics of the  $H_2$  oxidation reaction on the Pt electrocatalysts is much faster than that for the  $O_2$  reduction reaction, the cell impedance was mainly dominated by the cathodic impedance for the  $O_2$  reduction reaction. The  $CPE_a$  and  $CPE_c$  represent a constant phase element.

Table 1 lists the fitting data from the EIS. Theoretically, the proton conductivity of each doped AB-PBI membrane should be constant in all the cases because there is no significant difference of the PA doping level as well as GDL, membrane and the clamping

pressure for each MEA, which can be proved by the relative constant ohmic resistance for the cell prepared by GDEs. Nevertheless, when the Pt loading was low (0.2 and 0.3 mg cm<sup>-2</sup>), CCM-based MEAs showed lower ohmic resistances than that for GDE-based MEAs with same Pt loading due to the good CL/membrane interface contact resulting from the catalyst directly depositing on the membrane. In the case of increasing Pt loading (0.5 and 0.8 mg cm<sup>-2</sup>), although the CCM method was helpful to strengthening the contact between the CL and the membrane, too much Pt loading will make the CL thicker. The membrane may not absorb enough PA from the GDLs, resulting in lower membrane proton conductivity, which may offset the reduction from the superior interface contact, causing a similar (e.g. at 0.5 mg cm<sup>-2</sup>) or higher (e.g. at 0.8 mg cm<sup>-2</sup>) cell ohmic resistance. Meanwhile, it is found that some irregular dots appear at the low frequency range of the spectrum for the MEAs prepared by CCM method, which attributes to the gas transfer resistance for a thick CL. Jespersen et al. [29]

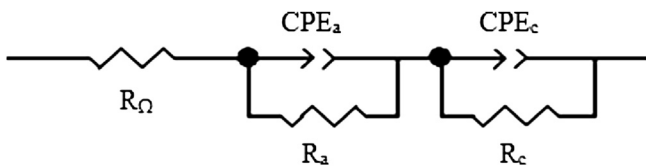


Fig. 5. Equivalent circuit used to fit the experimental data in Fig. 4.

Table 1

Fitted impedance parameters of the single cells prepared by CCM and GDE.

MEA	CCM				GDE			
	0.2	0.3	0.5	0.8	0.2	0.3	0.5	0.8
$R_\Omega$ ( $\Omega$ cm <sup>2</sup> )	0.313	0.331	0.442	0.502	0.421	0.438	0.446	0.441
$R_a$ ( $\Omega$ cm <sup>2</sup> )	0.245	0.070	0.139	0.329	0.110	0.213	0.127	0.160
$R_c$ ( $\Omega$ cm <sup>2</sup> )	0.414	0.570	0.626	0.556	1.223	0.630	0.194	0.205

discussed the each composition of the resistance in detail. They suggested that the gas transfer resistance mainly depends on the diffusion of oxygen in the channels of the bipolar plate, GDL and the electrodes, which is associated with the low frequency part of the spectrum. Lobato et al. [13] investigated the effect of carbon content in the microporous layer on the cell performance and found that higher carbon content is harmful to oxygen transfer properties because of some diffusion problems though a thicker layer. Hence, we consider that the thicker CL seems to make the diffusion of oxygen in the electrode become difficult and depress the cell performance.

As shown in Table 1, it can be observed that the CCM method is beneficial because the charge transfer resistance in the cathode ( $R_c$ ) is much lower than that for GDEs till the Pt loading increased to  $0.5 \text{ mg cm}^{-2}$ , indicating the interfacial impedance between the membrane and CL decreased by using CCM method. Tang et al. [7] believe that the CCM-based MEAs show faster charge transfer for ORR at the cathode and electrolyte interface and higher Pt utilization compared to GDEs. However, this situation undergoes a fundamental change with the Pt loading increasing. The MEAs prepared by GDEs may keep a better pore structure of CL, so  $R_c$  of GDEs are lower than those of CCMs when using higher Pt loadings for the anodes and cathodes. These variation tendencies are reflected on the cell performance. EIS results prove that CCMs have more efficient electrochemical active layer than the GDEs under a low Pt loading level.

Fig. 6 compares the cyclic voltammograms of the MEAs made from CCM and GDE with difference Pt loadings, respectively. The

ECSA can be calculated from the area of hydrogen desorption peak observed on cyclic voltammograms, which represents the Pt utilization of the cell. The electrochemical surface area of the Pt catalyst was calculated by the following formula (1), in which  $Q$  represents the hydrogen desorption charge on the electrode.

$$\text{ECSA} \left( \text{m}^2 \text{g}^{-1} \text{Pt} \right) = \frac{Q \left( \text{C cm}^{-2} \right)}{210 \times 10^4 \left( \mu \text{C cm}^{-2} \text{Pt} \right) \times \text{Pt loading} \left( \text{mg cm}^{-2} \right)} \quad (1)$$

As can be seen in Fig. 6, the cell prepared by CCM method shows noteworthy larger ECSA when only  $0.2 \text{ mg cm}^{-2}$  Pt was used in the CL, while a broad and weak desorption peak is observed for GDE-based MEA with same Pt loading. The ECSA is high up to  $23.6 \text{ m}^2 \text{g}^{-1} \text{Pt}$ , which is almost 3 times as much as that of prepared by GDE with the same Pt loading. As we know, the electrochemical reactions only occur at the three-phase boundaries, where the electrolyte, Pt/C catalyst and fuel all contact together in the MEA. The quality of the three-phase boundary depends significantly on the MEA fabrication technique and other important parameters, such as the catalyst loading and electrolyte loading [9]. Su et al. [6] also considered that the ECSA depends on the structure of the CL, as well as the distribution of the electrolyte. By using CCM method, a thin CL direct contact with the membrane, which results in an abundant the three-phase boundary. When the Pt loading was low ( $0.2$  and  $0.3 \text{ mg cm}^{-2}$ ), CCM-based MEAs showed high ECSA values due to the good CL/membrane interface contact, consequently high

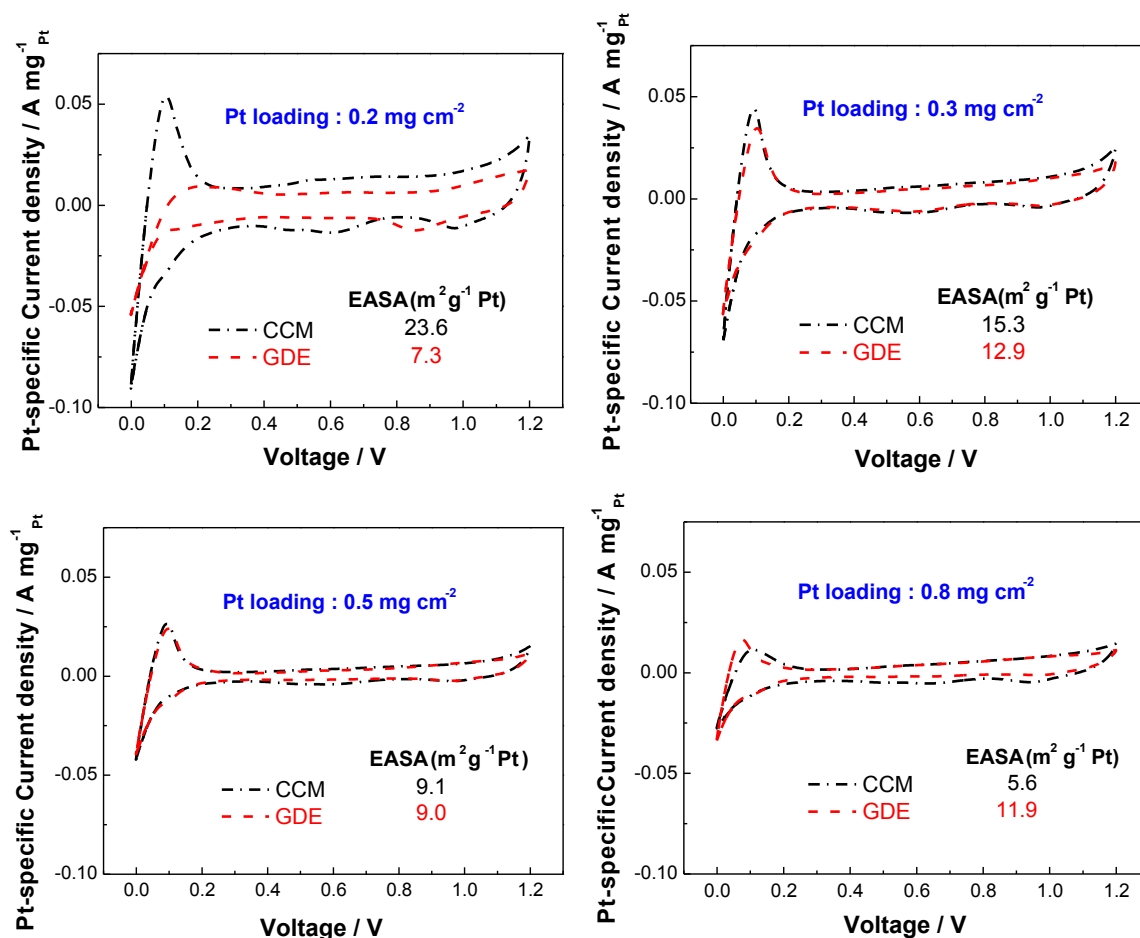


Fig. 6. Cyclic voltammograms of the MEAs prepared by CCM and GDE.

Pt utilization. However, when the CLs of the CCM-MEAs are thick ( $0.5$  and  $0.8 \text{ mg cm}^{-2}$  Pt loading), the membrane may not absorb enough PA from the GDLs, resulting in low Pt utilization in CL/membrane interface where the electrochemical reaction mainly occurs, which may offset the advantage from the superior interface contact, causing a similar ECSA value with the  $0.5 \text{ mg cm}^{-2}$  Pt loading GDE. In contrast, more Pt electrocatalyst penetrate into the pores of the GDL and is wasted, which amounts to reducing the Pt utilization. However, with increasing the Pt loading, the ECSA of MEA prepared by CCM sharply decreases, due to too much catalyst to increase the thickness of the CL and therefore PA diffusion in the CL become difficult and insufficient. We think the main reason is the different PA diffusion direction in the GDE and CCM. When the Pt loading is low, the CL is thin, PA distribution in the CL should be similar for both GDE and CCM, and then CCM has higher ECSA due to the better CL/membrane interface. When the Pt loading is high, the CL is thick, PA distribution in the GDE-CL/membrane interface should be better than that in CCM-CL/membrane interface due to the shorter PA diffusion distance. The CL/membrane interface is the place where the electrochemical reaction mainly occurs, the better PA distribution in this region of the GDEs with thick CL then showed similar ( $0.5 \text{ mg cm}^{-2}$  Pt) or higher ( $0.8 \text{ mg cm}^{-2}$  Pt) ECSA than the CCMs with same Pt loadings. It further demonstrates that the CCM method is advisable when utilizing a low Pt loading, making more Pt surface available and better three-phase boundary in the CL.

#### 4. Conclusions

MEAs developed by a novel CCM method were evaluated for the application on the AB-PBI based HT-PEMFC. Under an usual operating conditions ( $160^\circ\text{C}$ ,  $\text{H}_2/\text{Air}$ , ambient pressure), the maximum Pt-specific power density of the MEA prepared by CCM method was  $760 \text{ mW mg}^{-1}$  Pt and the limiting current density was as high as  $850 \text{ mA cm}^{-2}$ . The Pt-specific power density ratio of MEA prepared by CCM to that by GDE can reach up to 1.7 when the Pt loading is  $0.3 \text{ mg cm}^{-2}$  for the cathode. EIS studies show that the ohmic resistance and the cathode charge transfer resistance significantly decreased by using CCM method compared with the GDEs at low Pt loadings. CV results reveal that CCM can expand the three-phase boundary and enhance the Pt utilization efficiency of high temperature PEMFCs. Although the cell performance needs to be further optimized in this work, the CCM method was considered a promising way for the fabrication of low Pt loading and high Pt utilization MEAs for HT-PEMFC applications.

#### Acknowledgements

This work is supported by Hydrogen and Fuel Cell Technologies RDI Programme (HySA), funded by the Department of Science and Technology in South Africa (project KP1-S01). Financial support from the NRF Free-standing Postdoctoral Fellowship (Grant No: 88347) is also acknowledged.

#### References

- [1] Q. Li, J.O. Jensen, R.F. Savinell, N.J. Bjerrum, *Prog. Polym. Sci.* 34 (2009) 449–477.
- [2] Q. Li, R. He, J.O. Jensen, N.J. Bjerrum, *Fuel Cells* 4 (2004) 147–159.
- [3] L.W. Zhang, S.R. Chae, Z. Hendren, J.S. Park, M.R. Wiesner, *Chem. Eng. J.* 204 (2012) 87–97.
- [4] H. Su, T.-C. Jao, S. Pasupathi, B.J. Bladergroen, V. Linkov, B.G. Pollet, *J. Power Sources* 246 (2014) 63–67.
- [5] H. Su, S. Pasupathi, B.J. Bladergroen, V. Linkov, B.G. Pollet, *J. Power Sources* 242 (2013) 510–519.
- [6] H. Su, S. Pasupathi, B. Bladergroen, V. Linkov, B.G. Pollet, *Int. J. Hydrogen Energy* 38 (2013) 11370–11378.
- [7] H. Tang, S. Wang, S.P. Jiang, M. Pan, *J. Power Sources* 170 (2007) 140–144.
- [8] T. Suzuki, S. Tsushima, S. Hirai, *Int. J. Hydrogen Energy* 36 (2011) 12361–12369.
- [9] S. Thanasilp, M. Hunsom, *Fuel* 89 (2010) 3847–3852.
- [10] P. Mazur, J. Soukup, M. Paidar, K. Bouzek, *J. Appl. Electrochem.* 41 (2011) 1013–1019.
- [11] M. Mamlouk, K. Scott, *Int. J. Energy Res.* 35 (2011) 507–519.
- [12] M. Mamlouk, K. Scott, *Int. J. Hydrogen Energy* 35 (2010) 784–793.
- [13] J. Lobato, P. Cañizares, M.A. Rodrigo, D. Úbeda, F.J. Pinar, J.J. Linares, *Fuel Cells* 10 (2010) 770–777.
- [14] A.D. Modestov, M.R. Tarasevich, V.Y. Filimonov, A.Y. Leykin, *J. Electrochem. Soc.* 156 (2009) B650–B656.
- [15] H. Su, H. Liang, B.J. Bladergroen, V. Linkov, B.G. Pollet, S. Pasupathi, *J. Electrochem. Soc.* 161 (2014) F506–F512.
- [16] H.A. Gasteiger, J.E. Panels, S.G. Yan, *J. Power Sources* 127 (2004) 162–171.
- [17] H. Su, L. Xu, H. Zhu, Y. Wu, L. Yang, S. Liao, H. Song, Z. Liang, V. Birss, *Int. J. Hydrogen Energy* 35 (2010) 7874–7880.
- [18] H. Liang, L. Zheng, S. Liao, *Int. J. Hydrogen Energy* 37 (2012) 12860–12867.
- [19] X. Leimin, L. Shijun, Y. Lijun, L. Zhenxing, *Fuel Cells* 9 (2009) 101–105.
- [20] H. Liang, D. Dang, W. Xiong, H. Song, S. Liao, *J. Power Sources* 241 (2013) 367–372.
- [21] Y.-H. Cho, S.-K. Kim, T.-H. Kim, Y.-H. Cho, J.W. Lim, N. Jung, W.-S. Yoon, J.-C. Lee, Y.-E. Sung, *Electrochem. Solid-State Lett.* 14 (2011) B38–B40.
- [22] C. Wannek, I. Konradi, J. Mergel, W. Lehnert, *Int. J. Hydrogen Energy* 34 (2009) 9479–9485.
- [23] A. Chandan, M. Hattenberger, A. El-Kharouf, S.F. Du, A. Dhir, V. Self, B.G. Pollet, A. Ingram, W. Bujalski, *J. Power Sources* 231 (2013) 264–278.
- [24] M.L. Perry, J. Newman, E.J. Cairns, *J. Electrochem. Soc.* 145 (1998) 5–15.
- [25] C.-T. Liu, M.-H. Chang, *Int. J. Electrochem. Sci.* 8 (2013) 3687–3695.
- [26] J. Lobato, P. Cañizares, M.A. Rodrigo, J.J. Linares, F.J. Pinar, *Int. J. Hydrogen Energy* 35 (2010) 1347–1355.
- [27] J. Lobato, P. Cañizares, M.A. Rodrigo, J.J. Linares, D. Úbeda, F.J. Pinar, *Fuel Cells* 10 (2010) 312–319.
- [28] T.E. Springer, T.A. Zawodzinski, M.S. Wilson, S. Gottesfeld, *J. Electrochem. Soc.* 143 (1996) 587–599.
- [29] J.L. Jespersen, E. Schaltz, S.K. Kaer, *J. Power Sources* 191 (2009) 289–296.